Hindawi
Advances in Materials Science and Engineering
Volume 2021, Article ID 9385917, 8 pages
https://doi.org/10.1155/2021/9385917

Research Article

Submicron SiO_2 Powder: Characterization and Effects on Properties of Cement-Free Iron Ditch Castables

Shuiming Cheng,[1] **Huizhong Zhao**,[2] **Yu Wang**,[3] **Jianxiu Wei**,[4] **Jinfeng Chen**,[4] **Wei Cai**,[4] **and Han Zhang**[3]

[1]*The State Key Laboratory of Refractories and Metallurgy, Wuhan University of Science & Technology, Wuhan Research Institute of Metallurgy Construction Co. Ltd of MCC Group, Wuhan, China*
[2]*Wuhan University of Science and Technology, Wuhan, China*
[3]*The State Key Laboratory of Refractories and Metallurgy, Wuhan University of Science and Technology, Wuhan, China*
[4]*Wuhan Research Institute of Metallurgy Construction Co. Ltd of MCC Group, Wuhan, China*

Correspondence should be addressed to Han Zhang; wustzh@163.com

Received 25 April 2021; Revised 1 July 2021; Accepted 5 August 2021; Published 20 August 2021

Academic Editor: Aniello Riccio

Copyright © 2021 Shuiming Cheng et al. This is an open access article distributed under the Creative Commons Attribution License, which permits unrestricted use, distribution, and reproduction in any medium, provided the original work is properly cited.

Submicron materials are those with particle size diameters between 0.1 and 1 μm. Submicron SiO_2 generally refers to SiO_2 powder with a $D_{90} < 1$ μm (D_{90} refers to the particle size distribution exhibited by the sample and corresponds, in this case, to 90% of the particles not exceeding a diameter of 1 μm). In this study, a new type of cement-free iron ditch castable was prepared using dense corundum and silicon carbide as the primary raw materials with submicron SiO_2 powder as the binder. The effects of submicron SiO_2 powder content on the bulk density, apparent porosity, linear rate of change, compressive strength, and bending strength were investigated. The mechanism of action of the submicron SiO_2 powder was also investigated by analyzing its microstructure and particle size distribution. The results revealed that (1) the submicron SiO_2 powder can be used as the sole bonding agent in the preparation of cement-free iron ditch castables; (2) in comparison to traditional castables, the cement-free castable developed in this study demonstrated strong service performance and high-temperature bending strength.

1. Introduction

The iron ditch in a blast furnace forms a fundamental component in the ironmaking process. The vast majority of blast furnace casts worldwide use Al_2O_3–SiC–C iron ditch castables and pure calcium aluminate cement as the bonding agent [1–3]. However, the high-temperature performance of such castables declines due to the introduction of CaO in calcium aluminate cement [4–6]. This shortcoming cannot be optimized irrespective of the purity of the refractory raw materials. In addition, during the process of fabricating cement-bonded iron ditch castables and as a result of strong basic properties of cement, the comprising hydroxide ions can dissolve metal aluminum to produce aluminum hydroxide, which can cause metal aluminum powder to react with water to produce a large amount of hydrogen; this leads to porosity and even cracking of the material. Moreover, the bonding system containing cement also limits the introduction of additives such as Si_3N_4 [7] into the matrix, which is beneficial in improving the iron slag resistance properties and high-temperature performance. Thus, to solve this problem, refractory workers have carried out extensive research on cement-free combinations of iron ditch castables, and the general method of fabrication entails replacing pure calcium aluminate cement with silica sol or hydraulic hydrated alumina [8]. However, the applicability of silica sol is limited [9, 10] due to the disadvantages such as the reduced early strength exhibited by iron ditch castables bonded using silica sol while the time available for construction is severely limited and there is the high susceptibility to freezing in winter. In addition, its application offers no clear advantage over cement-incorporated iron trench castables [11, 12].

Iron ditch castables combined with hydraulic hydrated alumina exhibit not only low strength but also poor stability. Particularly, the speed of hydration is strongly dependent on temperature; as an example, more time and higher temperatures are required to eliminate water crystals, which can produce cracks and burst, thus affecting the structural density of the constructed body [13–16].

To meet the demands of intensified smelting operation in blast furnaces, there is an urgent need to develop a cement-free castable for iron ditch with excellent construction and service performance.

In this study, a new type of high-purity submicron SiO_2 powder was characterized, and its effects on the properties of Al_2O_3–SiC–C iron ditch castables were investigated. The use of a submicron SiO_2 powder as the sole bonding agent in the preparation of iron ditch castables was examined. This provides a novel concept for the study of cement-free iron ditch castable bonding systems.

2. Characterization of SiO_2 Powder

2.1. Particle Size and Morphology Analysis. Figure 1 shows the particle size (Mastersizer 2000, Malvern, UK) and morphology (JEM-2100UHR STEM/EDS, JEOL, Japan) of the submicron SiO_2 powder used in the experiment. As can be seen in the particle size distribution diagram in Figure 1(a), the particle size distribution range was narrow, ranging from 0.1 to 1.0 μm, with $D_{50} = 0.242\ \mu$m. Figure 1(b) shows a transmission electron microscope image of the submicron SiO_2 powder; the particle morphology was spherical, further confirmation that it was indeed submicron powder material.

Smaller particle sizes of the powder material are associated with higher specific surface areas and higher proportion of surface atoms, which tends to increase the reactivity and surface energy of the powder material. The number of atoms on the surface of the powder material is equal to the total number of atoms in the powder, which can be calculated by solving the following equation:

$$\begin{aligned} S &= \frac{(4/3)\pi\left(R^3 - r^3\right)/a^3}{(4/3)\pi R^3/a^3}, \\ &= 1 - \left(1 - \frac{a}{R}\right)^3, \\ &= 1 - \left(1 - \frac{2a}{D}\right)^3. \end{aligned} \tag{1}$$

In equation (1), R is the average particle radius, D is the particle size, and a is the lattice constant; $r = R - a$.

The lattice constant (a) for SiO_2 is 4.9133 Å (0.49133 nm), and the interatomic distance was set to be 0.3 nm. For the calculation, a in equation (1) was set to be 0.79 nm, and the percentage of atoms on the surface of the powder material, i.e., S, was calculated to be 2.35%, indicating that although the powder has a certain degree of reactivity, the activity is not strong. It should be noted that the submicron SiO_2 powder adopts an amorphous morphology, and the calculation results given in equation (1) are used as reference rather than absolute calculation results.

The silicon atoms, 3S and 3P, in SiO_2 were hybridized with SP3. There are 4 mol of Si–O bonds in 1 mol of SiO_2; thus, the basic structural unit is a tetrahedron. Each silicon atom is bound to four oxygen atoms; there is a silicon atom in the center and an oxygen atom at the four vertices. There are also six silicon atoms and six oxygen atoms in the smallest ring. Many of these tetrahedrons are connected by an oxygen atom at the top corners, and each oxygen atom is shared by two tetrahedrons, i.e., each oxygen atom is connected to two silicon atoms. SiO_2 is a three-dimensional network structure composed of a silicon atom and an oxygen atom at a ratio of 1 : 2.

The bulk density of the powder material was determined to be 0.31 g/cm^3, and the specific surface area was 26.53 m^2/g. Ten grams of the powder was uniformly dispersed in 100 g of deionized water. Following this was a 30 min period of ultrasonic dispersion; the dispersion solution was determined to have an acidic pH value of 3.51 as measured by a pH meter (Mettler-Toledo FE-28-Standard, manufactured by Mettler-Toledo International Trading (Shanghai) Co., Ltd), whereas the pH value of the aqueous dispersion solution of general silicon powder was determined to be approximately 7. This indicates that the high-purity submicron SiO_2 powder used in this experiment has a certain solubility in water that allows it to form a true solution of SiO_2 in its molecular dispersion state [17–19], i.e., monomolecular silicic acid (H_4SiO_4). H_4SiO_4 is unstable, and the two internal hydroxyl groups are dehydrated and decomposed into metasilicic acid (H_2SiO_3), as described by equations (2)–(4). Metasilicic acid is a weak acid with a steady ionization constant of 2×10^{-10} (under 25°C), which can ionize H^+; thus, the dispersion system of submicron SiO_2–H_2O is acidic.

$$SiO_2 + 2H_2O \longrightarrow H_4SiO_4, \tag{2}$$

$$H_4SiO_4 \longrightarrow H_2SiO_3 + H_2O, \tag{3}$$

$$H_2SiO_3 \longrightarrow HSiO_3^- + H^+. \tag{4}$$

Monomolecular silicic acid is soluble in water, but it gradually associates into bimolecular and trimolecular units in the solution, eventually forming an insoluble multimolecule polymer. The resulting colloid is referred to as silicic acid sol, which is commonly known as silica sol. This is the theoretical basis for using a silicon micropower-water system as a binder for unshaped refractory materials.

2.2. Chemical and Phase Composition Analysis. The submicron SiO_2 powder is a pure white powder; its chemical composition (ARL Perform'X, Thermo Scientific, USA) is described in Table 1, and phase composition is shown in Figure 2.

As can be seen in Table 1, the purity of this submicron SiO_2 was as high as 99.9%, indicating extremely low impurity content. Thus, it is a high-purity submicron powder.

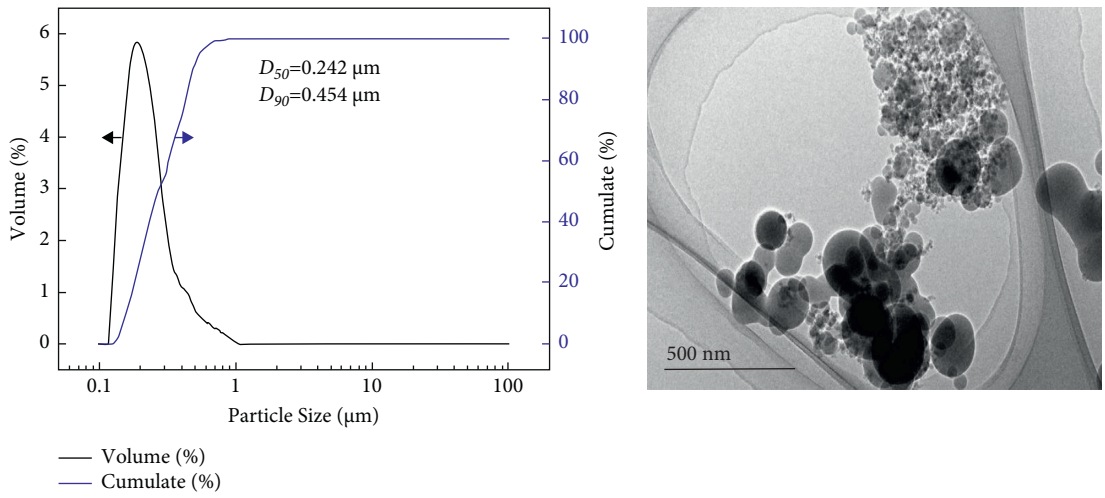

Figure 1: Particle size (a) and morphology (b) of SiO_2 powder.

Table 1: Chemical composition of submicron ultrahigh-purity SiO_2 powder (wt.%).

SiO_2	Al_2O_3	Fe_2O_3	CaO	MgO	Na_2O	K_2O	TiO_2	P	C
99.9	0.01	0.02	0.01	0.01	0.01	0.01	0.003	0.006	0.01

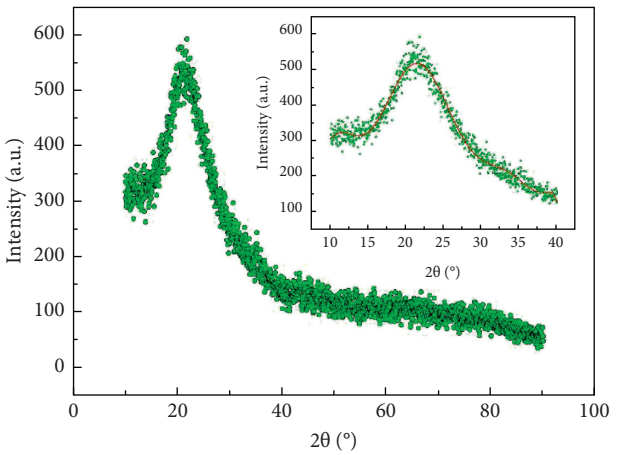

Figure 2: X-ray diffraction patterns of submicron high-purity SiO_2 powder.

Figure 2 shows the X-ray powder diffraction (X'Pert Pro, Philips, Netherlands, Cu target, 40 kV and 40 mA) of the submicron SiO_2 powder. Within the diffraction angle range of 10–90°, only one diffuse scattering amorphous peak was observed near $2\theta = 21.3°$. This further confirms that the SiO_2 powder used in this experiment was a high-purity amorphous submicron powder.

3. Application of Submicron SiO_2 Powder in Cement-Free Iron Ditch Castable

3.1. Raw Materials and Sample Ratio. The main raw materials used in the experiment were tabular alumina, w (Al_2O_3) = 99.07%, SiC, w (SiC) = 98.12%, spherical asphalt, w (C) = 56.21%, dense corundum powder, w (Al_2O_3) = 99.56%, and w (Na_2O) = 0.08%. The experimental formulations are presented in Table 2.

3.2. Sample Preparation and Performance Testing. The ingredients used in this study are listed in Table 2. After the mixture was dry mixed for 60 s, a certain volume of water was added; the flow value of all mixtures was controlled to approximately 170 mm by measuring the flow value of the mixture several times.

The flow value of the mixture was tested according to YB/T 5202.1–2003 (Black Metallurgy Industry Standard of the People's Republic of China). A shaking table was used to vibrate the mixture and obtain strip samples of 40 mm × 40 mm × 160 mm; then, the samples were cured under 25°C for 24 h to facilitate demolding. After demolding, the samples were naturally dried at 25°C for 24 h before being subjected to one of the following drying regimens: 110°C × 24 h, 1000°C × 3 h, and 1450°C × 3 h (high-temperature treatment).

The bulk density and apparent porosity of the samples subjected to 1450°C for 3 h were tested in accordance with GB/T 2997–2015 (National Standards of the People's Republic of China); the compressive strengths of the samples that were dried and heat-treated at different temperatures were tested in accordance with GB/T 5072–2008; the flexural strength of the samples that were dried and heat-treated at different temperatures was tested in accordance with GB/T 3001–2017. Additionally, the high-temperature (1400°C × 1 h) flexural strength of the samples dried in ambient air was tested in accordance with GB/T 3002–2017.

Table 2: Formulations for the experiment.

Materials and content (*wt*)/(%)	Particle size range	A	B	C	D	E	F	G
Tabular alumina	0.1–8 mm	60	60	60	60	60	60	60
SiC	0.5–1 mm	18	18	18	18	18	18	18
Spherical asphalt	0.1–1 mm	3	3	3	3	3	3	3
Water-reducing agent	—	0.1	0.1	0.1	0.1	0.1	0.1	0.1
Metal silicon	≤0.05 mm	1.5	1.5	1.5	1.5	1.5	1.5	1.5
Submicron SiO_2 powder	$D_{90} = 0.454\,\mu m$	3	4	5	6	7	8	9
Dense corundum powder	≤0.06 mm	14.4	13.4	12.4	11.4	10.4	9.4	8.4
Water addition (flow value = 170 mm)	—	4.6	4.0	3.6	3.4	3.3	3.2	3.2

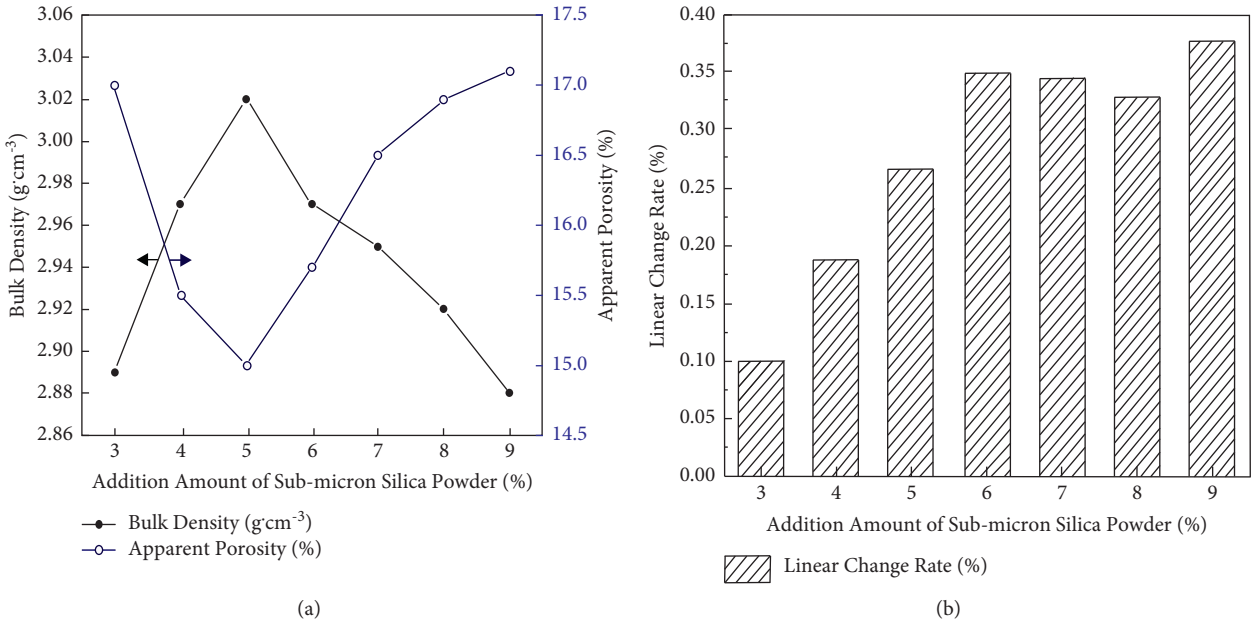

Figure 3: Physical properties of samples sintered at 1450°C for 3 h.

4. Results and Discussion

4.1. Effects of Submicron SiO_2 Powder Content on the Density of Samples. The physical properties of the samples treated at different temperatures are shown in Figure 3. As shown in Figure 3(a), the samples that were sintered at 1450°C for 3 h were observed to have the highest bulk density and lowest apparent porosity when the submicron SiO_2 powder addition amount was 5%. Additionally, the linear rate of change for the samples treated at 1450°C for 3 h increased with increasing submicron SiO_2 powder content, shown in Figure 3(b).

4.2. Effects of Submicron SiO_2 Powder Content on the Mechanical Properties. Figure 4 shows the mechanical properties exhibited by samples treated at various temperatures. As shown in Figure 4, the samples dried at 110°C for 24 h exhibited greater compressive and flexural strength when the submicron SiO_2 powder content was between 6 and 8 wt%. Samples sintered at 1000°C for 3 h exhibited greater compressive and flexural strength when the submicron SiO_2 powder content was between 5 and 8 wt%. Moreover, the compressive and flexural strength exhibited by the samples sintered at 1450°C for 3 h, as well as the high-temperature flexural strength exhibited by the samples sintered at 1400°C for 1 h; both reached their maximum values when the submicron SiO_2 powder content was 5 wt%. This may be due to the highest density and the best direct bonding degree of the sample.

4.3. Scanning Electron Microscopy (SEM) Analysis. Figure 5 shows the scanning electron microscopy (SEM, JSM-6610, JEOL, Japan) images of samples with different submicron SiO_2 powder contents that have been sintered at 1450°C for 3 h. As can be seen in Figure 5, the sample with 3 wt% of submicron SiO_2 powder had higher porosity and weak aggregate/matrix bonding. Increasing the submicron SiO_2 powder content to 5 wt% resulted in stronger matrix bonding and a clear increase in the density of the sample. However, further increase in the submicron SiO_2 powder content to 7 wt% resulted in the occurrence of pores in the matrix. This may be due to the formation of Si–OH–Si bonds, which occurred as a result of the hydration of a greater volume of SiO_2, that produced pores during the process of dehydration when the samples were sintered at

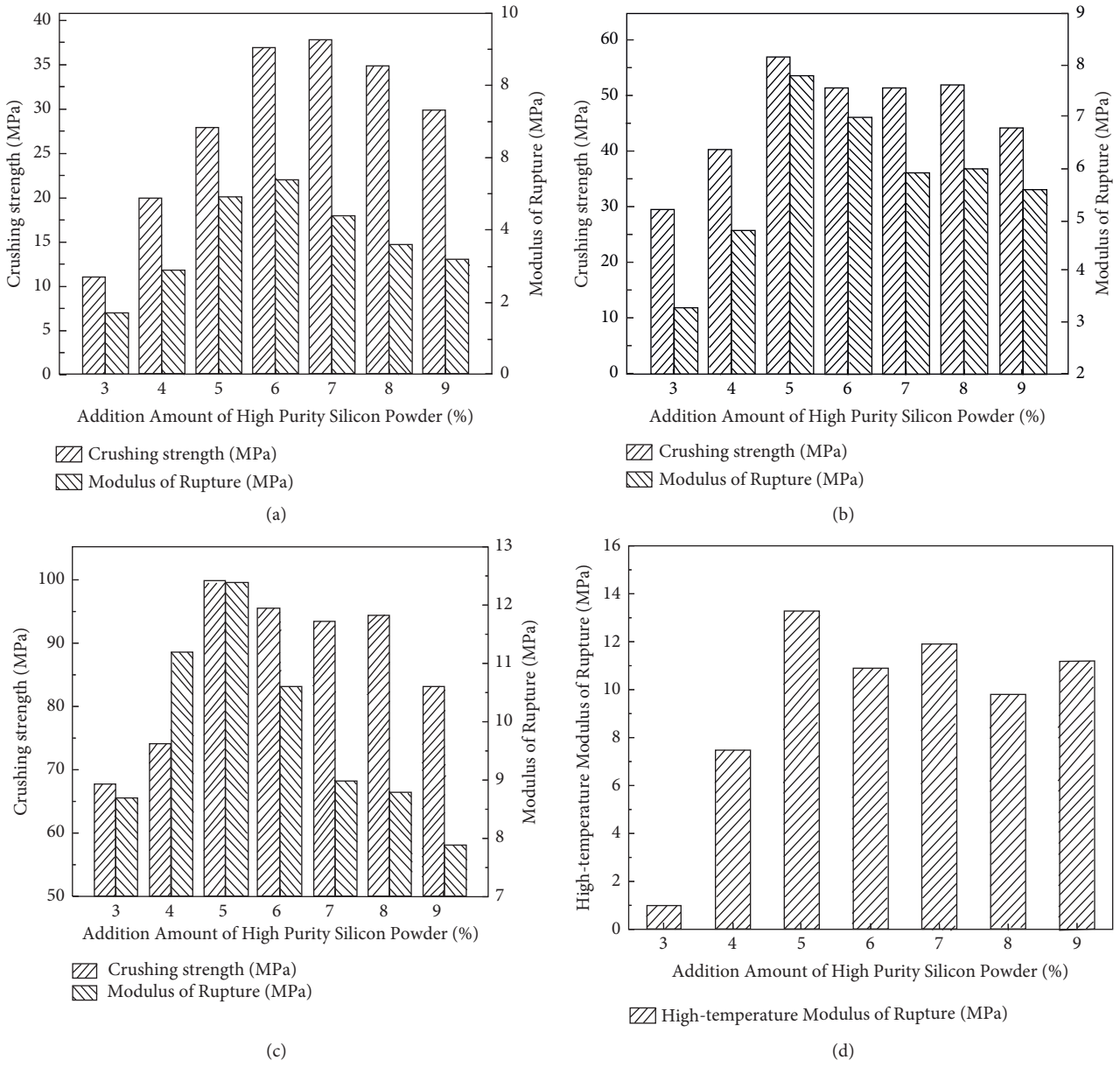

Figure 4: Mechanical properties of specimens treated at different temperatures: (a) compressive and flexural strength of samples dried at 110°C for 24 h; (b) compressive and flexural strength of samples sintered at 1000°C for 3 h; (c) compressive and flexural strength of samples sintered at 1450°C for 3 h; (d) high-temperature flexural strength of samples sintered at 1400°C for 1 h.

high temperatures. Further increasing the submicron SiO_2 powder to 9 wt% resulted in further weakened matrix bonding and more pores.

In addition, combined with the water addition amount (the flow value of all mixtures was controlled to approximately 170 mm shown in Table 2), it is shown that the submicron SiO_2 powder exhibits a strong micropowder filler function. At present, the D_{90} and D_{50} of most condensed SiO_2 micropowders in China are approximately 7.599 μm and 0.416 μm, respectively, whereas the D_{90} and D_{50} of the submicron SiO_2 powders used in this study were 0.454 μm and 0.242 μm, respectively. As shown in Figure 1, having smaller-sized particles corresponds to an increased interspace filling of the powder, which leads to higher reactivity.

The samples that were 4 wt% submicron SiO_2 powder were found to have high demolding strength after being cured for 24 h. Additionally, increasing the content of submicron SiO_2 powder to 5 wt% corresponded to an increase in the viscosity of the castable slurry; however, the medium-high temperature strength of the sample did not significantly increase. Further increase in the submicron SiO_2 powder content to 6 wt% did not coincide with a significant decrease in the water content of the castable; however, the speed of solidification was found to have accelerated. Finally, when the submicron SiO_2 powder content reached 7-8 wt%, the viscosity of the castable was found to improve, while the volume of water required to meet the construction condition also increased, the required

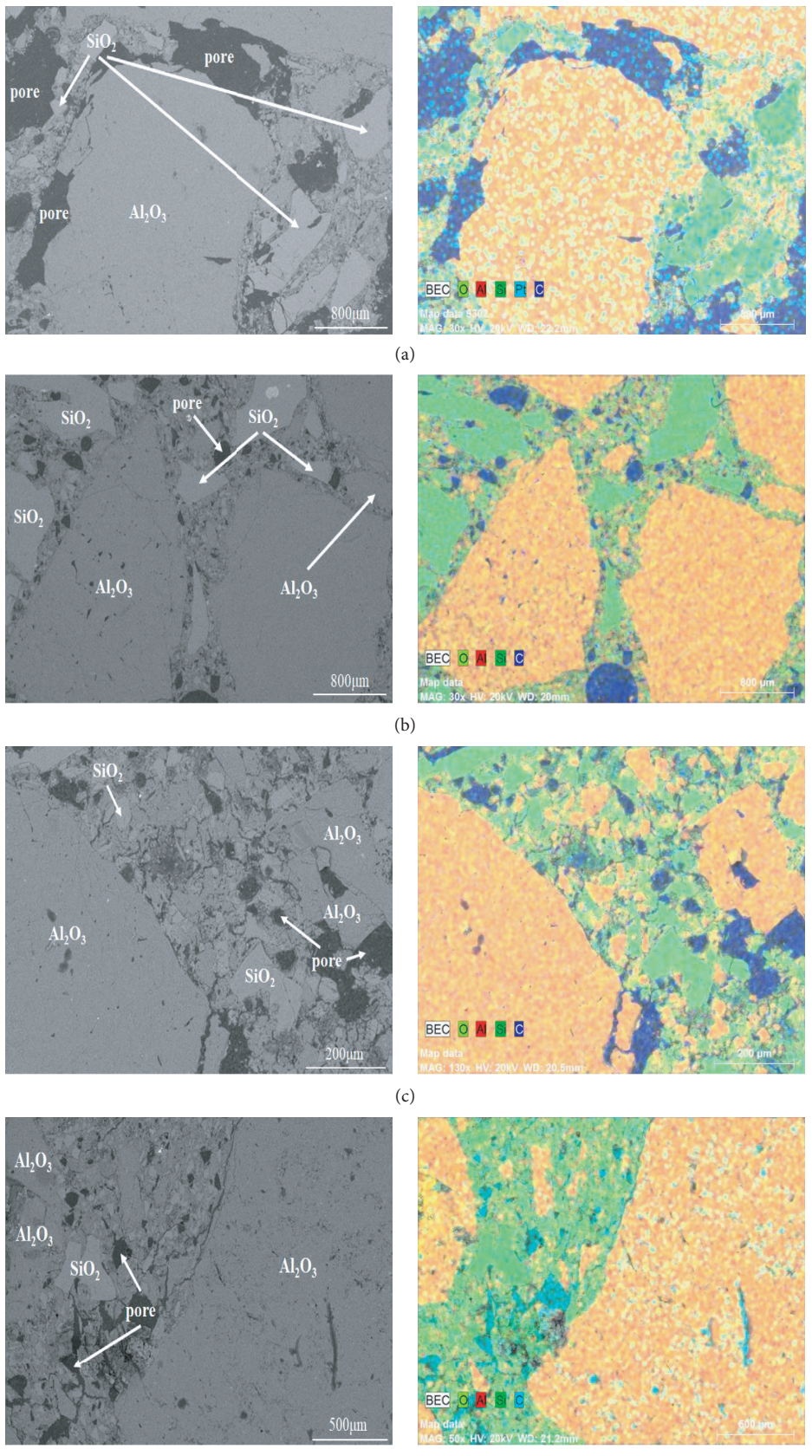

Figure 5: SEM images of samples with different submicron SiO_2 powder contents: (a) 3 wt%; (b) 5 wt%; (c) 7 wt%; (d) 9 wt%.

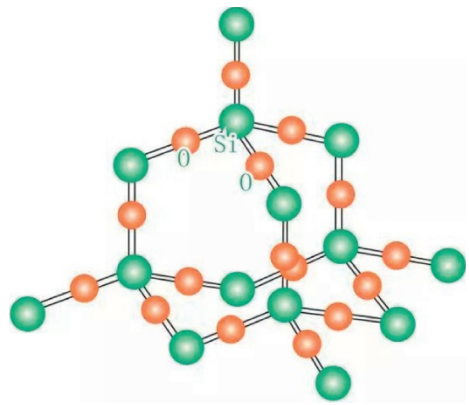

Figure 6: Unit cell of silica.

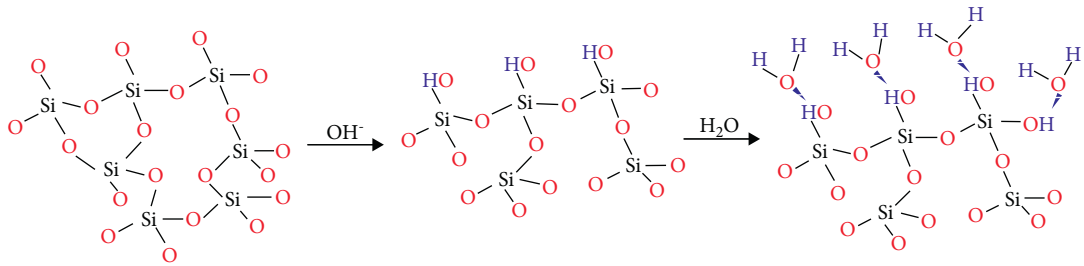

Figure 7: Schematic of the processes of amorphous SiO_2 hydroxylation and water adsorption [20].

stirring time was significantly lengthened, and there was no significant increase in the dried strength of the sample. Thus, the optimum submicron SiO_2 powder content in an iron ditch castable was determined to be within the range between 4 and 6 wt%.

Amorphous SiO_2 has a short-range ordered structure, as shown in Figure 6. When water is added to the iron ditch castable, the amorphous SiO_2 reacts with the OH^- of the water on the surface, resulting in the hydroxylation of SiO_2. Then, the hydroxylated SiO_2 adsorbs water; during this time, the adsorbed water on the surface of the aggregate and matrix quenches the SiO_2, forming a three-dimensional network bonding in the castable body. This structure is known to be associated with high strength; thus, the proposed castable has high strength. This process is illustrated in Figure 7.

The experimental results show that the submicron SiO_2 powder can be used as a binder for cement-free iron ditch castables, indicating that the realization of cement-free iron ditch castables is possible.

5. Conclusions

(1) The SiO_2 powder used in this experiment was a high-purity submicron powder material.

(2) The submicron SiO_2 powder can be used as the sole bonding agent for the production of iron ditch castables, thereby offering a cement-free option for iron ditch castables.

(3) As compared with conventional castables, the cement-free iron ditch castable developed in this study had a significantly lower water content (minimum of 3.2%). Moreover, the high-temperature flexural strength was significantly higher, with the maximum exceeding 13 MPa. The optimum submicron SiO_2 powder content for the type of iron ditch castable developed in this study was determined to be within the range between 4 and 6 wt%.

Data Availability

The data used to support the findings of this study are included within the article.

Conflicts of Interest

The authors declare that they have no conflicts of interest.

Acknowledgments

This work was supported by the National Natural Science Foundation of China (No. 51804233).

References

[1] Y. Li, H. Zhao, H. Zhang et al., "Enhancement and explosion-proof mechanism of aluminum fiber addition in Al_2O_3-SiC-C castables for iron runner," *Ceramics International*, vol. 45, no. 17, Article ID 22723, 2019.

[2] P. Zhou, X. Qiu, Z. Luo, X. Liu, S. Zhang, and Q. Jia, "Effect of firing atmosphere on the microstructure and properties of Al_2O_3-SiC-C castables," *Ceramics International*, vol. 47, no. 10, Article ID 14280, 2021.

[3] V. Pilli and R. Sarkar, "Effect of spinel content on the properties of Al_2O_3-SiC-C based trough castable," *Ceramics International*, vol. 42, no. 2, pp. 2969–2982, 2016.
[4] J. Shan, Y. Li, N. Liao, M. Nath, L. Pan, and S. Sang, "Critical roles of synthetic zeolite on the properties of ultra-low cement-bonded Al_2O_3-SiC-C castables," *Journal of the European Ceramic Society*, vol. 40, no. 15, pp. 6132–6140, 2020.
[5] G. Ye and T. Troczynski, "Hydration of hydratable alumina in the presence of various forms of MgO," *Ceramics International*, vol. 32, no. 3, pp. 257–262, 2006.
[6] C. Gogtas, H. F. Lopez, and K. Sobolev, "Role of cement content on the properties of self-flowing Al_2O_3 refractory castables," *Journal of the European Ceramic Society*, vol. 34, no. 5, pp. 1365–1373, 2014.
[7] A. Chen, Y. Fu, Y. Mu et al., "Oxidation resistance of andalusite-bearing Al_2O_3–SiC–C castables containing reduced anti-oxidant," *Ceramics International*, vol. 47, no. 10, Article ID 14579, 2021.
[8] V. Pilli and R. Sarkar, "A comparative study on bonding systems in alumina-silicon carbide-carbon-based trough castable," *Ironmaking and Steelmaking*, vol. 43, no. 9, pp. 705–711, 2016.
[9] S. Hossein badiee and S. Otroj, "Non-cement refractory castables containing nano-silica: performance, microstructure, properties," *Ceramics-Silikáty*, vol. 53, no. 4, pp. 297–302, 2009.
[10] S. Otroj, M. A. Bahrevar, F. Mostarzadeh et al., "The effect of deflocculants on the self-flow characteristics of ultra low-cement castables in Al_2O_3-SiC-C system," *Ceramics International*, vol. 31, no. 5, pp. 647–653, 2005.
[11] G. Liu, X. Jin, W. Qiu et al., "The effect of microsilica on the oxidation resistance of Al_2O_3–SiC–SiO_2–C castables with Si and B_4C additives," *Ceramics International*, vol. 42, no. 1, pp. 251–262, 2016.
[12] X. Fan, K. Jiao, J. Zhang et al., "Study on physicochemical properties of Al_2O_3-SiC-C castable for blast furnace," *Ceramics International*, vol. 45, no. 11, Article ID 13903, 2019.
[13] R. Salomão and V. C. Pandolfelli, "The role of hydraulic binders on magnesia containing refractory castables: calcium aluminate cement and hydratable alumina," *Ceramics International*, vol. 35, no. 8, pp. 3117–3124, 2009.
[14] F. A. O. Valenzuela and V. C. Pandolfelli, "Drying behavior of hydratable alumina-bonded refractory castables," *Journal of the European Ceramic Society*, vol. 24, no. 5, pp. 797–802, 2004.
[15] N. Xu, Y. Li, S. Li et al., "Hydration mechanism and sintering characteristics of hydratable alumina with microsilica addition," *Ceramics International*, vol. 45, no. 11, Article ID 13780, 2019.
[16] D. Chen, H. Gu, A. Huang et al., "Enhancement of bonding network for silica sol bonded SiC castables by reactive micropowder," *Ceramics International*, vol. 43, no. 12, pp. 8850–8857, 2017.
[17] M. Kawaguchi, "Stability and rheological properties of silica suspensions in water- immiscible liquids," *Advances in Colloid and Interface Science*, vol. 278, Article ID 102139, 2020.
[18] T. Oertel, U. Helbig, F. Hutter et al., "Influence of amorphous silica on the hydration in ultra-high performance concrete," *Cement and Concrete Research*, vol. 58, pp. 121–130, 2014.
[19] I. Gunnarsson and S. Arnórsson, "Amorphous silica solubility and the thermodynamic properties of H_4SiO_4 in the range of 0° to 350°C at Psat," *Geochimica et Cosmochimica Acta*, vol. 64, no. 13, pp. 2295–2307, 2000.
[20] L. Khouchaf, K. Boulahya, P. P. Das et al., "Study of the microstructure of amorphous silica nanostructures using high-resolution electron microscopy, electron energy loss spectroscopy, X-ray powder diffraction, and electron pair distribution function," *Materials*, vol. 13, p. 4393, 2020.